World Journal of Gastroenterology

Online Submissions: http://www.wjgnet.com/esps/
wjg@wjgnet.com
doi:10.3748/wjg.v18.i30.3962

World J Gastroenterol 2012 August 14; 18(30): 3962-3976
ISSN 1007-9327 (print) ISSN 2219-2840 (online)

ORIGINAL ARTICLE

Increased expression of chondroitin sulphate proteoglycans in rat hepatocellular carcinoma tissues

Xiao-Li Jia, Si-Yuan Li, Shuang-Suo Dang, Yan-An Cheng, Xin Zhang, Wen-Jun Wang, Clare E Hughes, Bruce Caterson

Xiao-Li Jia, Shuang-Suo Dang, Yan-An Cheng, Xin Zhang, Wen-Jun Wang, Department of Infectious Diseases, The Second Affiliated Hospital of Medical School of Xi'an Jiaotong University, Xi'an 710004, Shaanxi Province, China
Si-Yuan Li, Clare E Hughes, Bruce Caterson, Connective Tissue Biology Laboratories, Division of Pathophysiology and Repair, School of Biosciences, Cardiff University, Cardiff, Wales CF10 3AX, United Kingdom
Si-Yuan Li, The Institute of Endemic Disease, Medical School of Xi'an Jiaotong University, Xi'an 710061, Shaanxi Province, China
Author contributions: Jia XL, Dang SS and Cheng YA designed the research; Jia XL, Li SY, Zhang X and Wang WJ performed the experiments; Li SY and Hughes CE provided the reagents; Jia XL, Li SY, Hughes CE and Caterson B analyzed the data; Jia XL, Dang SS, Li SY, Hughes CE and Caterson B wrote the manuscript.
Supported by The National Natural Science Foundation of China, No. 30471982 (to Dang SS and Cheng YA); and Arthritis Research UK, No. 18331 (to Hughes CE and Caterson B)
Correspondence to: Shuang-Suo Dang, MD, PhD, Department of Infectious Disease, The Second Affiliated Hospital of Xi'an Jiaotong University, 157 Xiwu Road, Xi'an 710004, Shaanxi Province, China. dang212@126.com
Telephone: +86-29-87679688 Fax: +86-29-87678599
Received: February 13, 2012 Revised: March 28, 2012
Accepted: April 13, 2012
Published online: August 14, 2012

Abstract

AIM: To investigate the expression of chondroitin sulphate proteoglycans (CSPGs) in rat liver tissues of hepatocellular carcinoma (HCC).

METHODS: Thirty male Sprague Dawley rats were randomly divided into two groups: control group (n = 10) and HCC model group (n = 20). Rats in the HCC model groups were intragastrically administrated with 0.2% (w/v) N-diethylnitrosamine (DEN) every 5 d for 16 wk, whereas 0.9% (w/v) normal saline was administered to rats in the control group. After 16 wk from the initiation of experiment, all rats were killed and livers were collected and fixed in 4% (w/v) paraformaldehyde. All tissues were embedded in paraffin and sectioned. Histological staining (hematoxylin and eosin and Toluidine blue) was performed to demonstrate the onset of HCC and the content of sulphated glycosaminoglycan (sGAG). Immunohistochemical staining was performed to investigate the expression of chondroitin sulphate (CS)/dermatan sulphate (DS)-GAG, heparan sulphate (HS)-GAG, keratan sulphate (KS)-GAG in liver tissues. Furthermore, expression and distribution of CSPG family members, including aggrecan, versican, biglycan and decorin in liver tissues, were also immunohistochemically determined.

RESULTS: After 16 wk administration of DEN, malignant nodules were observed on the surface of livers from the HCC model group, and their hepatic lobule structures appeared largely disrupted under microscope. Toluidine blue staining demonstrated that there was an significant increase in sGAG content in HCC tissues when compared with that in the normal liver tissues from the control group [0.37 ± 0.05 integrated optical density per stained area (IOD/area) and 0.21 ± 0.01 IOD/area, $P < 0.05$]. Immunohistochemical studies demonstrated that this increased sGAG in HCC tissues was induced by an elevated expression of CS/DS (0.28 ± 0.02 IOD/area and 0.18 ± 0.02 IOD/area, $P < 0.05$) and HS (0.30 ± 0.03 IOD/area and 0.17 ± 0.02 IOD/area, $P < 0.01$) but not KS GAGs in HCC tissues. Further studies thereby were performed to investigate the expression and distribution of several CSPG components in HCC tissues, including aggrecan, versican, biglycan and decorin. Interestingly, there was a distinct distribution pattern for these CSPG components between HCC tissues and the normal tissues. Positive staining of aggrecan, biglycan and decorin was localized in hepatic membrane and/or pericellular matrix in normal liver tissues; however, their expression was

mainly observed in the cytoplasm, cell membranes in hepatoma cells and/or pericellular matrix within HCC tissues. Semi-quantitative analysis indicated that there was a higher level of expression of aggrecan (0.43 ± 0.01 and 0.35 ± 0.03, $P < 0.05$), biglycan (0.32 ± 0.01 and 0.25 ± 0.01, $P < 0.001$) and decorin (0.29 ± 0.01 and 0.26 ± 0.01, $P < 0.05$) in HCC tissues compared with that in the normal liver tissues. Very weak versican positive staining was observed in hepatocytes near central vein in normal liver tissues; however there was an intensive versican distribution in fibrosis septa between the hepatoma nodules. Semi-quantitative analysis indicated that the positive rate of versican in hepatoma tissues from the HCC model group was much higher than that in the control group (33.61% and 21.28%, $P < 0.05$). There was no positive staining in lumican and keratocan, two major KSPGs, in either normal or HCC liver tissues.

CONCLUSION: CSPGs play important roles in the onset and progression of HCC, and may provide potential therapeutic targets and clinical biomarkers for this prevalent tumor in humans.

Key words: Hepatocellular carcinoma; Proteoglycan; Chondroitin sulphate; Heparan sulphate; Keratan sulphate

Peer reviewers: Mark Pines, PhD, Institute of Animal Sciences, Volcani Center, PO Box 6, Bet Dagan 50250, Israel; Ralph Graeser, PhD, Group Leader, Molecular and Cellular Biology, ProQinase GmbH, Breisacher Str. 117, 79106 Freiburg, Germany

Jia XL, Li SY, Dang SS, Cheng YA, Zhang X, Wang WJ, Hughes CE, Caterson B. Increased expression of chondroitin sulphate proteoglycans in rat hepatocellular carcinoma tissues. *World J Gastroenterol* 2012; 18(30): 3962-3976 Available from: URL: http://www.wjgnet.com/1007-9327/full/v18/i30/3962.htm DOI: http://dx.doi.org/10.3748/wjg.v18.i30.3962

INTRODUCTION

Proteoglycans (PGs) are remarkably complex macromolecules consisting of one or more glycosaminoglycan (GAG) chains, which are covalently attached to different core proteins. Depending upon the structures of their GAG side-chains, PGs can be categorized as different groups such as heparan sulphate PGs (HSPGs), chondroitin/dermatan sulphate PGs (CS/DS PGs) and keratan sulphate PGs (KSPGs)[1]. According to their different structures of the core proteins, CS/DS PGs can be further categorized as large aggregating PGs (aggrecan, versican), and small leucine-rich PGs (biglycan and decorin), which have been found to be widely expressed in many tissues including liver.

CS/DS PGs are major components of the cell surface and extracellular matrix (ECM)[1,2]. They perform a myriad of functions ranging from structural roles in the ECM to control of growth factor gradients and the regulation of certain cell processes such as cell adhesion, growth, receptor binding, migration, and interactions with other ECM constituents[3-5]. These, especially the latter two functions, are largely mediated through specific interactions between their charged GAG chains and proteins such as growth factors, cytokines, chemokines, proteinases and their inhibitors[6,7]. In addition, emerging data have revealed that the core proteins of PGs can also form complexes with other proteins, such as integrins and regulate their signaling[7]. Because CS/DS PGs are at the crossroads of many signaling events and the abilities to regulate cell behaviors, they are being extensively investigated for their potential as therapeutic targets for cancers. What has become clear to date is that the functional effects of CS/DS PGs on cancers can range from stimulatory to inhibitory influences[5], depending on the core protein and GAG structures[1,8], the types and stages of cancers and the localizations of the tumors[9].

PGs have been found widespread and abundant in liver tissues[10]. Interestingly, in rats, fetal and early neonatal liver exhibits a completely different PG expression pattern when compared with adult liver tissues, where the synthesis of heparan sulphate (HS) comprises more than 80% and CS less than 5% of total GAGs[11]. In contrast, CS is the major type of GAG synthesized in fetal liver, representing above 50% of total sulfated GAG (sGAG). Moreover, the overall PG production in fetal liver is enhanced two-fold when compared with that in the adult liver tissues. Thus, the synthesis of CS is elevated nearly 30-fold in fetal liver as compared with the adult counterpart[12]. Immediately after birth CS formation decreases rapidly to the adult levels between the 10th and 15th day of postnatal life[13], whereas the production of HS is almost unchanged during perinatal liver development due to a relatively low fractional synthesis of HS GAG in fetal liver[12]. This phenomenon illustrates that CSPG synthesis and expression in liver tissues are cell-type dependent, and the undifferentiated liver cells trend to produce more CSPGs compared with the differentiated hepatocytes in the adult liver tissues.

Interestingly, the expression patterns of PGs including HSPGs and CSPGs are markedly changed under pathological conditions[14]. For example, PGs are abnormally expressed in a wide variety of malignant tumors[9]. In liver, hepatocellular carcinoma (HCC) and hepatic parenchyma adjacent to tumor contain abnormally higher concentrations of CS GAGs than the corresponding healthy tissues, but only with mild alteration in HS expression, indicating that the increase in CS GAGs is a characteristic abnormality in HCC tissues[15-17]. This indicates that the expression of CSPGs plays a pivotal role in the occurrence, progression and metastasis of HCC, and therefore CSPG expression may be a potential marker and treatment target for HCC.

In this study, the expression patterns of different CSPGs including aggrecan, versican, decorin, biglycan in

the liver tissue from a rat HCC model established using N-diethylnitrosamine (DEN) were investigated using histological and immunochemical staining analyses.

MATERIALS AND METHODS

All chemicals were obtained from Xi'an Chemical Reagent Factory (Xi'an, China) unless otherwise stated and were of analytical grade or better.

Animal model preparation

The rat HCC model experimentation was approved by the Animal Ethics Committee, Medical School of Xi'an Jiaotong University. Use of animals in this study was in accordance with the China National Institute of Health publication 85-23 "Guide for Care and Use of Laboratory Animals" (National Research Council, 1996). Thirty male Sprague Dawley rats weighing 248.18 ± 12.32 g (3-4 mo old) were purchased from the Laboratory Animal Center of Medical School, Xi'an Jiaotong University. Rats were acclimated for 7 d before experimentation. Rats were randomly divided into two groups: control group (n = 10) and HCC model group (n = 20). Rats in the HCC model group were intragastrically administrated with 0.2% (w/v) DEN (Sigma, United State) in saline (10 ng DEN per gram body weight) every 5 d for 16 wk, whereas 0.9% (w/v) normal saline was administered to the rats in the control group. All the rats had free access to distilled water. Electrolyte balance between the two groups was maintained through their common dietary food intake.

Sample collection

The weights of the rats were measured every week. After 16 wk from the initiation of the experiment, all the rats were killed under general anesthesia. Hepatic tissues were collected and fixed in 4% (w/v) paraformaldehyde in phosphate buffered saline (PBS, 0.16 mol/L NaCl, 0.003 mol/L KCl, 0.008 mol/L Na_2HPO_4, 0.001 mol/L KH_2PO_4, pH 7.3) immediately. The tissues were embedded in paraffin and sectioned at 8 μm thickness.

Histological staining

Sections were deparaffinized and hydrated and either stained with hematoxylin and eosin or Toluidine blue as previously described[18]. After dehydration, sections were mounted using DPX mounting medium (Thermo Fisher Scientific, Loughborough, United Kingdom). Representative regions were photographed under bright field optics using a Leica DMRB light microscope (Leica, Wetzlar, Germany) equipped with digital image acquisition.

Immunohistochemical staining

Immunohistochemical staining was performed using Mouse on Mouse™ Vectastain® Elite® ABC Kits (Vector labs, Peterborough, United Kingdom) according to the manufacturer's protocols. Briefly, sections were incubated with 0.3% (v/v) hydrogen peroxide for 30 min at room temperature to quench endogenous peroxidase activity. After blocking with mouse immunoglobulin (Ig) blocking reagent for 1 h at room temperature, sections were incubated with rat anti-Versican (Abcam, Cambridge, United Kingdom), mouse anti-Aggrecan, mouse anti-Decorin, mouse anti-Keratocan, mouse anti-Lumican, mouse anti-Biglycan (in house) primary antibodies[19] for 60 min, respectively. For the negative control, the primary antibody was replaced by PBS or 2 μg/mL mouse or rat IgG (DAKO, Ely, United Kingdom). Sections were then incubated with biotinylated goat anti-mouse or rat IgG for 30 min at room temperature. After washing, sections were incubated with Mouse on Mouse™ ABC reagent for 5 min. Sections were then visualized using Vector® NovaRED™ kit (Vector labs, Peterborough, United Kingdom) according to the manufacturer's protocols. Cell nucleuses were counterstained with hemotoxylin. After dehydration, sections were mounted using DPX mountaining medium. Representative regions were then photographed under bright field optics using a Leica DMRB bright field microscope (Leica, Wetzlar, Germany) equipped with digital image acquisition.

Semi-quantitative analysis for versican positive rate in liver tissues

Positive staining rate for versican in liver tissue sections was quantitatively analyzed. Sections of 4 liver tissues from 4 individual rats in each experimental group were taken for analysis. For each liver tissue specimen, three sections were randomly selected, and the positive and negative stained cells in these sections were counted using Image J software (NIH, United States). The percentage of positive cells was then calculated using the equation below: the percentage of positive cells = (positive stained cells)/(positive stained cells + negative stained cells) × 100%.

Semi-quantitative analysis for the intensity of positive staining in tissues

The intensity of positive staining in tissue sections was analyzed by integrated optical density (IOD) using the Image-Pro Plus 5.1 software (Media Cybernetics, United States) as described previously[20] with minor modification. Briefly, four 20 × TIFF-format images from four individual rats in each group were analyzed in a blinded manner. All of the images were taken using the same microscope and camera sets. Image-pro Plus software was used to calculate the average IOD per stained area (μm^2) (IOD/area) for positive staining.

Statistical analysis

Data were presented as mean ± SE, with samples derived from 4 animals in each group. D'Agostino and Pear omnibus normality test was used for normality and equal variances test. Student t test plus Bonferroni's post-test was carried out using GraphPad Prism 4.0 software (GraphPad Software Inc., California, United States). The comparisons of the staining results were performed only between rats from the HCC model and the control groups, but not between the tumor nodules and its adjacent normal liver

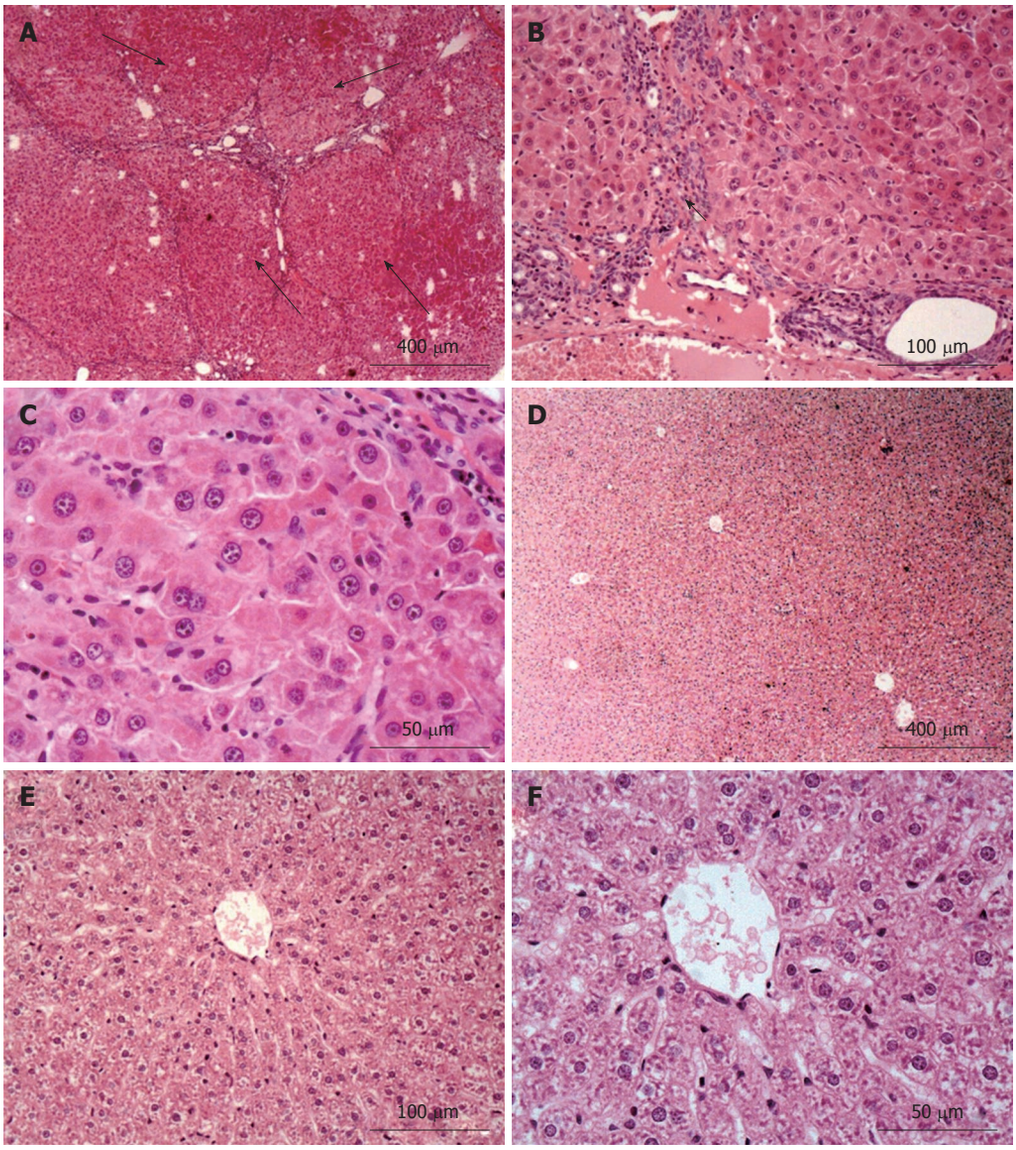

Figure 1 Hematoxylin and eosin staining results for liver tissues from the hepatocellular carcinoma model (A-C) and the control group (D-F). Normal liver structure and cell morphology were observed in the control group. However, apparent hepatoma nodules (long black arrows, A) and fibrosis (short black arrow, B) in the hepatocellular carcinoma model group were observed when compared with that in the control group.

tissues of rats from the same group. Differences were considered significant at $P < 0.05$.

RESULTS

Rat HCC model establishment

After 16 wk administration of DEN, malignant nodules were observed on the surface of the livers in the HCC model group but not in the control group. The average number of macroscopic nodules bigger than 3 mm and 5 mm on the surface of a single liver was 33.4 and 4.9, respectively, with the biggest nodule being approximately 1.5 cm × 1.0 cm × 0.8 cm (Table 1). H and E staining was used to identify and classify the cancerous nodules pathologically according to Edmondson *et al*[21]. As expected, the normal hepatic lobule structure was disrupted and hepatoma nodules (long black arrows) were evident in the tissues from the HCC model group (Figure 1A), which were separated by fibrosis septa (short black arrows, Figure 1B), suggesting fibrosis formation around the tumors. The differentiation of HCC cells was also investigated according to method described by Edmondson. All of the cancer cells in the HCC model group were classified as grade Ⅲ, and there was no hepatic plate-like structure present in the tumor tissues (Figure 1C). In contrast, there was no evidence of macroscopic tumor nodules in the livers from

Table 1 Number and size of malignant nodules in rat livers

Group	*n*	Nodules ⩾ 3 mm	Nodules ⩾ 5 mm	The biggest nodule (mm^3)
Control group	10	0	0	0
Model group	14	33.4 ± 7.9	4.9 ± 1.9	122.8

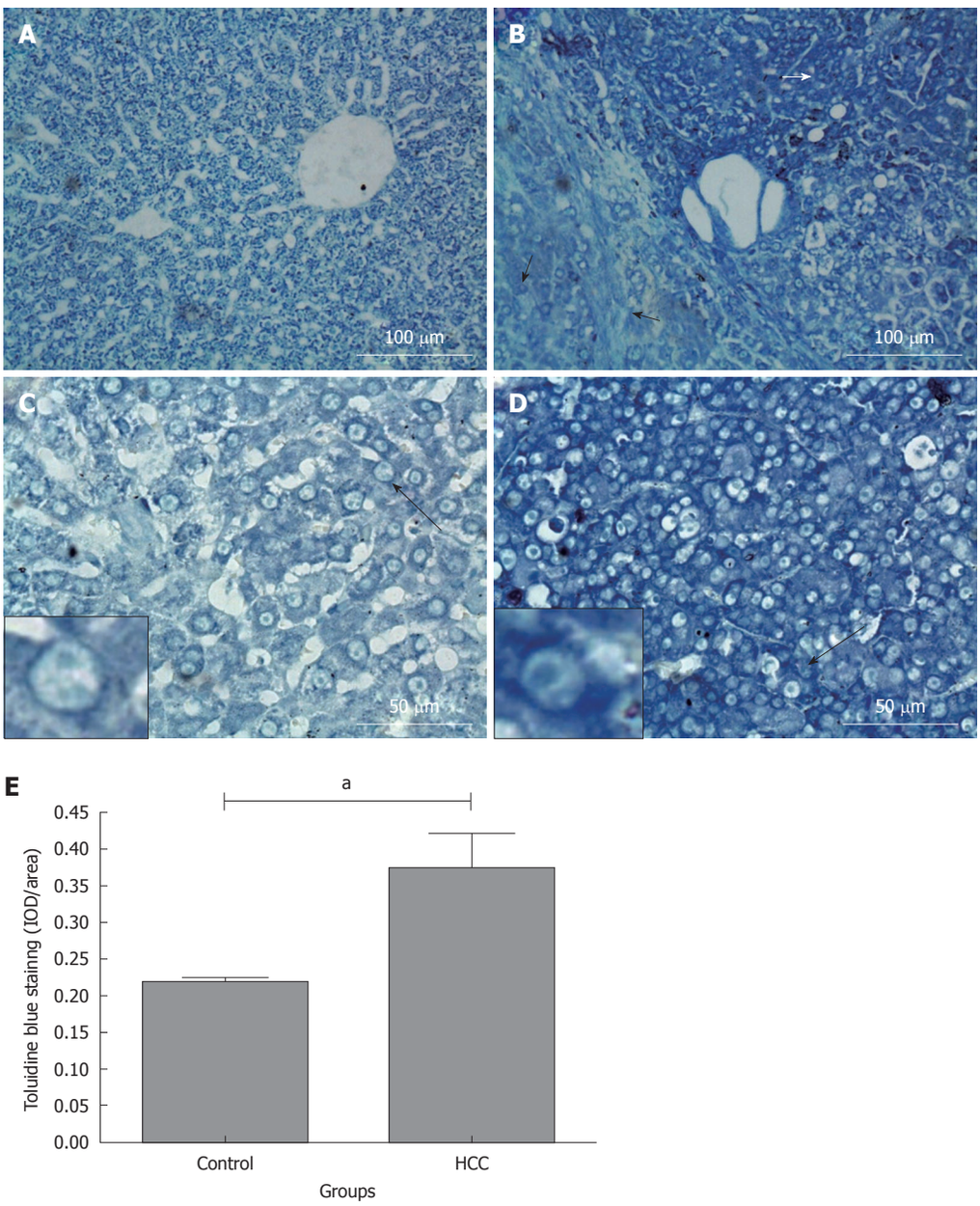

Figure 2 Toluidine blue staining in rat liver tissue sections. Rats were treated with N-diethylnitrosamine for 16 wk to establish a hepatocellular carcinoma (HCC) animal model. Sulphated glycosaminoglycan content in tissues were stained with Toluidine blue. A and C: Control group; B and D: HCC model group. Long black arrows: The cells are magnified in the small boxes. Short white arrow: Hepatoma tissues with intensive Toluidine blue staining; short black arrow: Weaker Toluidine blue staining fibrosis and "relative normal" liver tissues adjacent to the hepatoma nodules; E: Comparison of average integrated optical density (IOD) of toluidine blue staining in liver tissue between control and HCC model group ($^aP < 0.05$). IOD/area: **Integrated optical density per stained area**.

rats in the control group (Figure 1D), where a normal morphology was observed for hepatic cells, composing a normal liver tissue structure (Figure 1E and F). These results indicated the successful establishment of HCC in rats treated with DEN.

Increased sGAG content in HCC tissues

The contents of sGAG were investigated using Toluidine blue staining, which was evident in liver tissues from both control (Figure 2A and C) and HCC model groups (Figure 2B and D). Positive staining was found in the cytoplasm, cell membrane and/or pericellular matrix (Figure 2C and D; the cells identified by long black arrows are magnified in the small boxes). Noticeably, Toluidine blue staining in hepatoma tissues (white short arrow, Figure 2B) was stronger than that in the fibrosis and "relative normal liver tissue" (black short arrows, Figure 2B) adjacent to the tumor nodules. Semi-quantitative IOD analysis indicated that there was more Toluidine blue positive staining in the tissues from the HCC model group when compared with the tissues from the control group (0.37 ± 0.05 IOD/area and 0.21 ± 0.01 IOD/area, $P < 0.05$, Figure 2E). This finding demonstrates elevated sGAG content in HCC tissues compared to that in the normal liver tissues. To

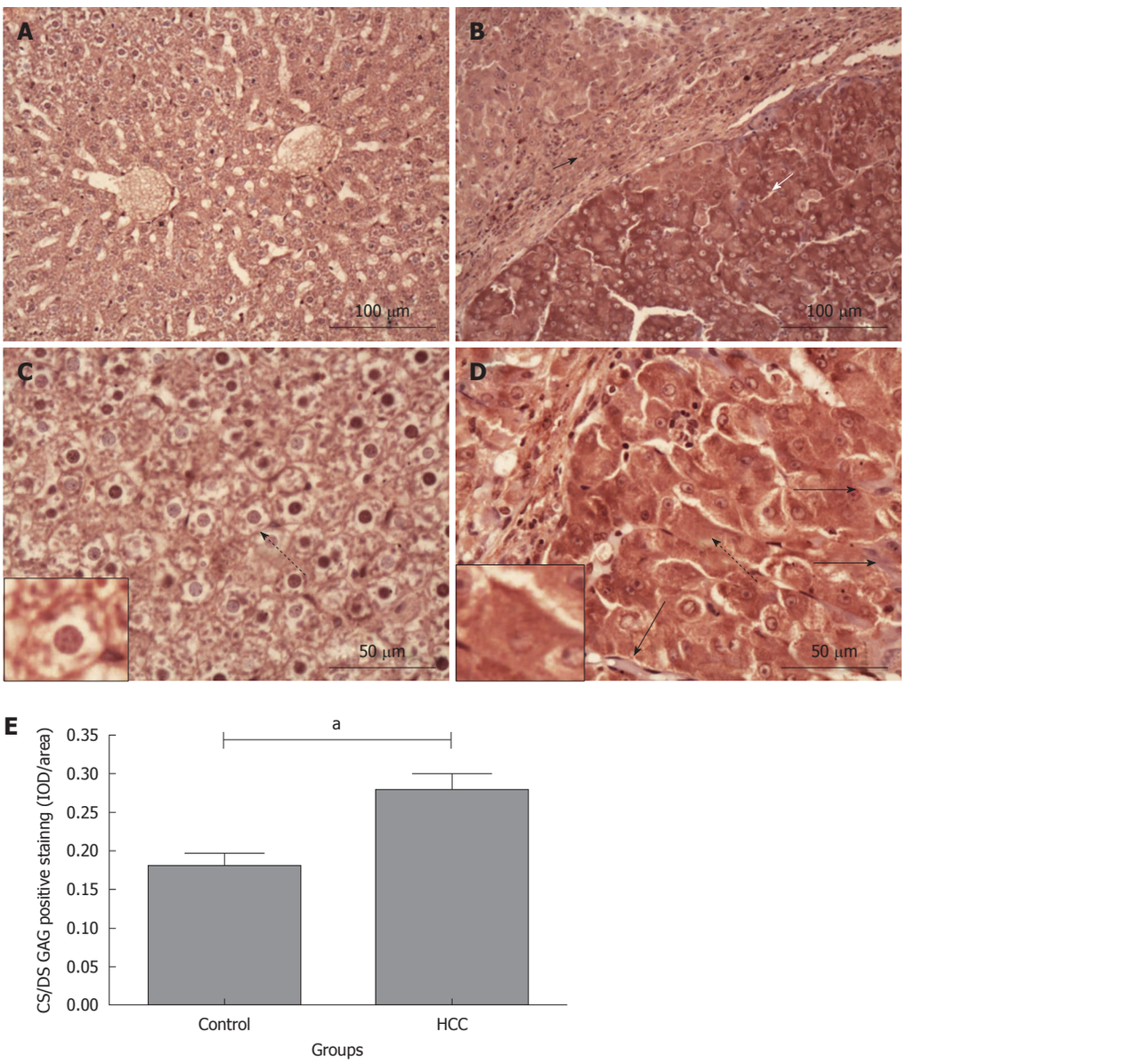

Figure 3 Chondroitin sulphate/dermatan sulphate glycosaminoglycan immunohistochemical staining in rat liver tissues. Chondroitin sulphate (CS)/dermatan sulphate (DS) sulphated glycosaminoglycan (sGAG) content in liver tissues was stained using 2B6 (+) antibody (dark red). A and C: Control group; B and D: Hepatocellular carcinoma (HCC) model group. Long black arrows: Perisinusoidal cells negatively stained by 2B6 antibody; dotted arrows: The cells are magnified in the small boxes; short white arrow: Hepatoma tissues with intensive CS/DS GAG staining; short black arrow: Weaker CS/DS GAG staining in fibrosis and "relative normal" liver tissues adjacent to the hepatoma nodules; E: Comparison of the average integrated optical density (IOD) in CS/DS GAG positive staining in liver tissues between the control and HCC model groups ($^{a}P < 0.05$). IOD/area: **Integrated optical density per stained area.**

further identify the specific expression of sGAG in HCC model tissue, immunohistochemical staining for CS/DS, HS and keratan sulphate (KS) GAG were performed.

Increased CS/DS GAG expression in HCC tissues

The expression of CS/DS GAG chains in normal and HCC tissues was investigated using 2B6 (+) monoclonal antibody[1,19]. As shown in Figure 3, positive staining for 4-sulphated CS/DS GAGs was observed on cell membranes and/or pericellular matrix in the normal liver tissues from the control group (Figure 3A and C; the cell identified with dotted arrow is magnified in the small box). In contrast, 2B6 (+) positive staining was observed in the cytoplasm, cell membrane and/or pericellular matrix (Figure 3B and D; the cell pointed with dotted arrow is magnified in the small box). The expression of 4-sulphated CS/DS GAGs was variable across the HCC tissues, with a stronger staining in the hepatoma nodules (white short arrow, Figure 3B) but a relative weaker staining in its adjacent tissues such as fibrous septa and relatively normal hepatocytes (black short arrow, Figure 3B). Interestingly, these variable distribution patterns in 4-sulphated CS/DS were also observed inside the hepatoma nodules, i.e., several perisinusoidal cells were negatively stained in CS/DS expression (Figure 3D, black long arrows), although most of the hepatoma cells were positively stained. Semi-quantitative IOD analysis for the intensity of positive staining indicated that there was more 4-sulphated CS/DS expres-

sions in the hepatoma nodules when compared with that in the normal tissues from the control group (0.28 ± 0.02 IOD/area and 0.18 ± 0.02 IOD/area, $P < 0.05$, Figure 3E).

Increased HS GAG staining in HCC tissues

We also investigated the expression of HS GAG chains in the tissues from rats in the control and HCC model groups. Similar to the CS/DS GAG staining, HS positive staining was evenly distributed across the normal liver tissue sections from the control group (Figure 4A and D) and mainly localized on the cell membrane and/or pericellular matrix (Figure 4D; the cell identified with a black short arrow is shown at a higher magnification in the small box). However, this "normal tissue" HS distribution pattern was altered and became uneven in the tissues obtained from rats in the HCC model group. In some hepatoma nodules, intensive HS positive staining was observed in the hepatoma cytoplasm, cell membrane, pericellular matrix and even in cell nuclei (Figure 4E; the cell identified with a black short arrow is shown at a higher magnification in the small box). There was no HS positive staining in the fibrous tissue septa (black long arrows; Figure 4B and E). Semi-quantitative IOD analysis indicated that there was a stronger HS staining in these hepatoma nodules than that in the normal liver tissues from the control group (0.30 ± 0.03 and 0.17 ± 0.02, $P < 0.01$, Figure 4G). However in some hepatoma nodules, a relative weaker HS positive staining was observed on the hepatoma cell membrane and/or pericellular matrix (Figure 4C and F; the cell identified with a black short arrow is shown at a higher magnification in the small box), similar to that observed in the normal liver tissues from the control group. In this case, there was no significant difference in the average density of HS positive staining between the HCC model and the control groups ($P = 0.1169$).

KS GAG expression was not altered in HCC tissues

KS is another important sGAG side chains attached to the core proteins of several matrix PGs. In contrast to the CS and HS GAG staining described above, the positive staining of KS GAG chains was weak and there was no difference between control and HCC model groups (data not shown).

Collectively, the results described above demonstrate that there is a significant elevation in the expression of CS/DS and HS but not KS GAG chains in the HCC model tissues when compared with the normal liver tissues. Therefore, we further investigated the expression patterns of different PG core proteins with CS GAGs, including aggrecan, versican, biglycan and decorin.

Increased aggrecan expression in HCC tissues

Aggrecan is a common CSPG found in many musculoskeletal tissues especially in hyaline articular cartilage. Interestingly, aggrecan expression in the liver at the gene level has been reported previously[14,22]. In this study, aggrecan expression in liver tissues was immunohistochemically investigated using a monoclonal antibody [anti-IGD (6B4)] recognizing the interglobular domain of aggrecan core protein[19,23]. Positive staining for aggrecan was observed in both control and HCC model groups (Figure 5A and B). However, their distribution patterns were different. In the control group where aggrecan positive staining was mainly localized on cell membrane and/or pericellular matrix (Figure 5C; the cell identified with a black short arrow is magnified in the small box). In contrast, there was more intensive aggrecan positive staining in hepatoma cytoplasm, cell membrane and/or pericellular matrix in the tissues from the HCC model group (Figure 5D; the cell identified with a black short arrow is magnified in the small box). Noticeably, there was no or very weak aggrecan positive staining in the fibrous tissue septa between hepatoma nodules (black long arrows, Figure 5B and D). Interestingly, the differences in staining intensity and patterns for aggrecan described above were also observed between the hepatoma tissues and its adjacent "relative normal liver tissues" (Figure 5E; the areas inside the black or red boxes are magnified on the left column). Semi-quantitative IOD analysis indicated that there was more aggrecan positive staining in the tissues from the HCC model group when compared with that in the control group (0.43 ± 0.01 IOD/area and 0.35 ± 0.03 IOD/area, $P < 0.05$, Figure 5F). These results demonstrated that DEN-induced HCC in rat liver increases the aggrecan expression in cells at the protein level, suggesting that there may be a correlation between HCC and aggrecan expression.

Increased versican expression in HCC tissues

Versican is another member of the large aggregating CSPGs family and its expression in rat liver tissues was also investigated by immunohistochemical staining. In contrast to the aggrecan staining, most of the hepatocytes were negatively stained for versican in the liver tissues from the control group (Figure 6A and D). However, a weak versican positive staining was observed on the cell membrane and/or pericellular matrix of some hepatocytes around the central vein (Figure 6D; the cell identified with a black short arrow is magnified in the small box). In the liver tissues from rats in the HCC model group, versican positive staining was observed in some hepatoma cells (Figure 6B and E), and mainly localized in the cytoplasm, cell membrane and/or pericellular matrix (Figure 6E; the cell identified with a black short arrow is magnified in the small box). Statistical analysis indicated that versican positive staining rate in the HCC model group was much higher than that in the control group (33.61% ± 4.90% and 21.28% ± 1.79%, $P < 0.05$, Figure 6G), although a large number of cells were still negatively stained. Interestingly, the strongest versican positive staining was observed in the pericellular matrix of fibrous tissue septa and portal areas (Figure 6C and F), indicating a different versican distribution pattern between the control and HCC model groups.

Increased biglycan expression in HCC tissues

In normal liver tissues, a moderate positive staining of biglycan was evenly distributed on hepatic membrane

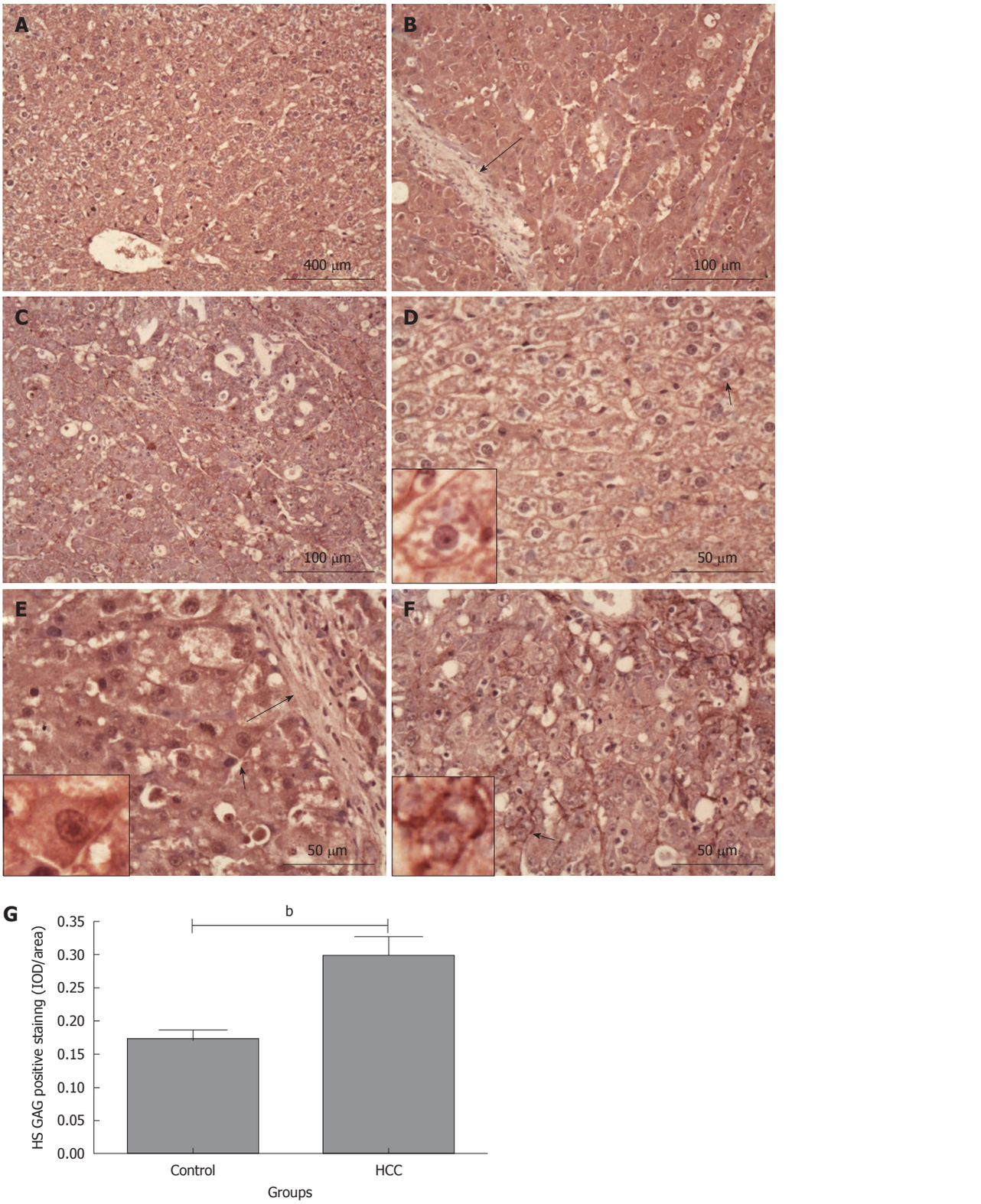

Figure 4 Heparan sulphate glycosaminoglycan staining in rat liver tissues. Heparan sulphate (HS) glycosaminoglycan (GAG) content in tissue was stained using 10E4 antibody (dark red). **A and D: Control group; B and E: Hepatocellular carcinoma (HCC) tissues with intensive HS GAG staining; C and F: HCC tissues with** relative weaker HS GAG staining. Long black arrows: Fibrous tissue septa; short black arrows: **The cells are magnified in the small boxes; G: Comparison of the average integrated optical density (IOD) in HS GAG positive staining in liver tissues between the control and HCC model groups ($^{b}P < 0.01$). IOD/area: Integrated optical density per stained area.**

and/or pericellular matrix in the liver tissues of rats from the control group (Figure 7A). There was limited positive staining in hepatocyte cytoplasm and nuclei (Figure 7C; the cell identified with a black short arrow is magnified in

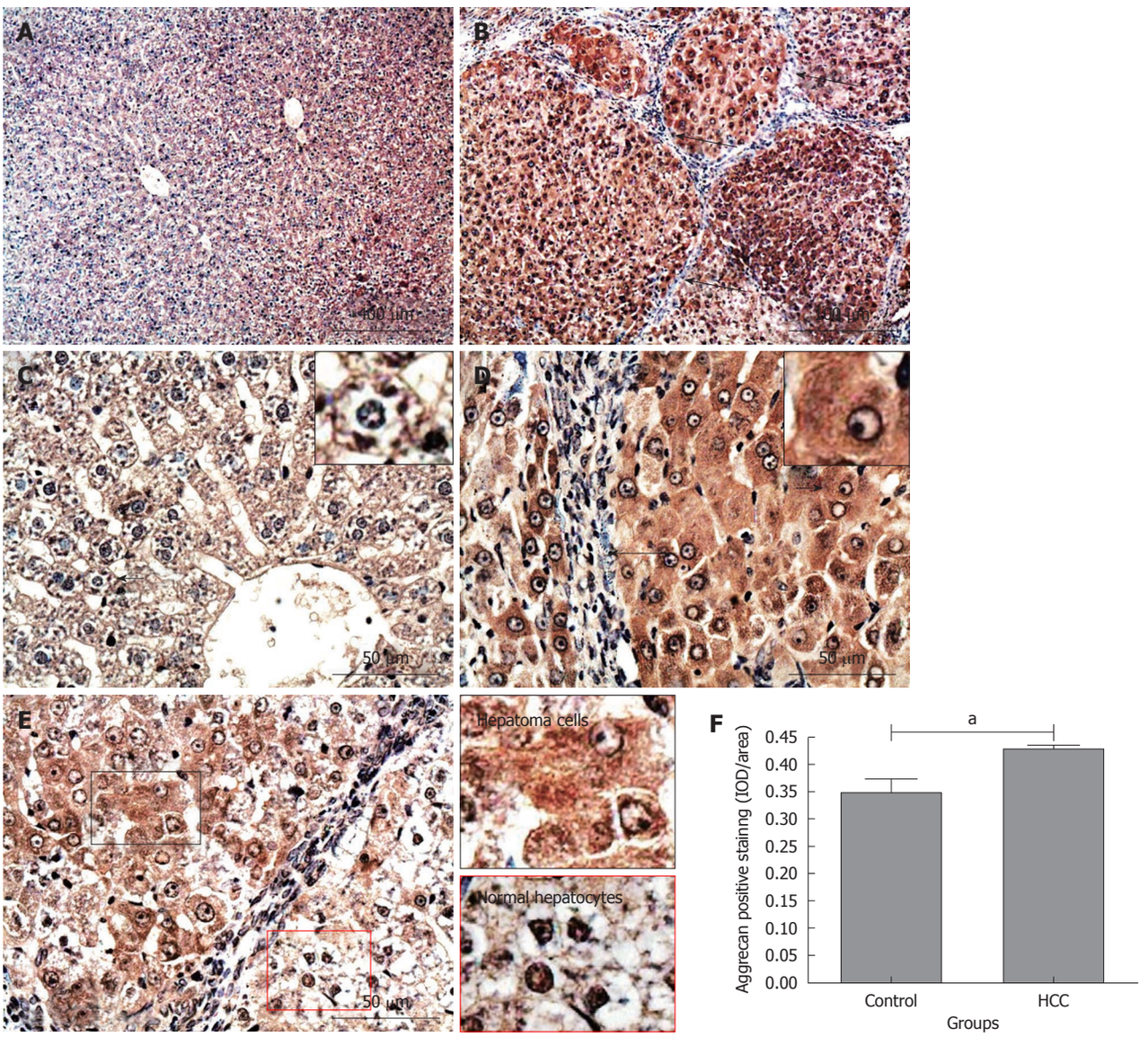

Figure 5 Immunochemical staining for aggrecan in rat liver tissues. Aggrecan positive staining was dark red. A and C: Control group; B, D and E: Hepatocellular carcinoma (HCC) model group. Long black arrows: **Fibrous tissue septa; short black arrows: The cells are magnified in the small boxes; E: Areas in black and red** boxes are magnified in left column; F: Comparison of the average integrated optical density (IOD) in aggrecan positive staining in liver tissues between the control and HCC model groups ($^{a}P < 0.05$). IOD/area: **Integrated optical density per stained area.**

the small box). In contrast, strong biglycan staining was observed in almost all hepatoma cells in tumor nodules from the HCC model group (Figure 7B). The staining was not only on the cell membrane and/or pericellular matrix but also in the cytoplasm (Figure 7D; the cell identified with a white short arrow is magnified in the small box). Interestingly, the differences in staining intensity and patterns for biglycan were also observed between hepatoma cells and its adjacent "relatively normal hepatocytes" (Figure 7E; the areas inside the black or red boxes are magnified on the left column). Semi-quantitative IOD analysis showed that there was significantly more biglycan expression in HCC tissues when compared with that in the normal liver tissues (0.32 ± 0.01 and 0.25 ± 0.01, $P < 0.001$, Figure 7F). There was no intensive biglycan staining in the portal areas and fibrous tissue septa between hepatoma nodules (white long arrow, Figure 7D).

Increased decorin expression in HCC tissues

Similarly to biglycan, decorin positive staining was evenly distributed on hepatic cell membrane and/or pericellular matrix across the whole liver tissue sections from the control group (Figure 8A and C; the cell identified with a black short arrow is magnified in the small box). In the HCC model tissues, intensive decorin positive staining was observed in almost all hepatoma cells (Figure 8B), mainly localized in the cytoplasm, cell membrane and/or pericellular matrix (Figure 8D; the cell identified with a black short arrow is magnified in the small box). This difference described above was also observed between hepatoma cells and its adjacent "relatively normal hepatocytes" (Figure 8E; the areas inside the black or red boxes are magnified on the left column). Semi-quantitative IOD analysis indicated that there was significantly more decorin expression in hepatoma nodules when compared

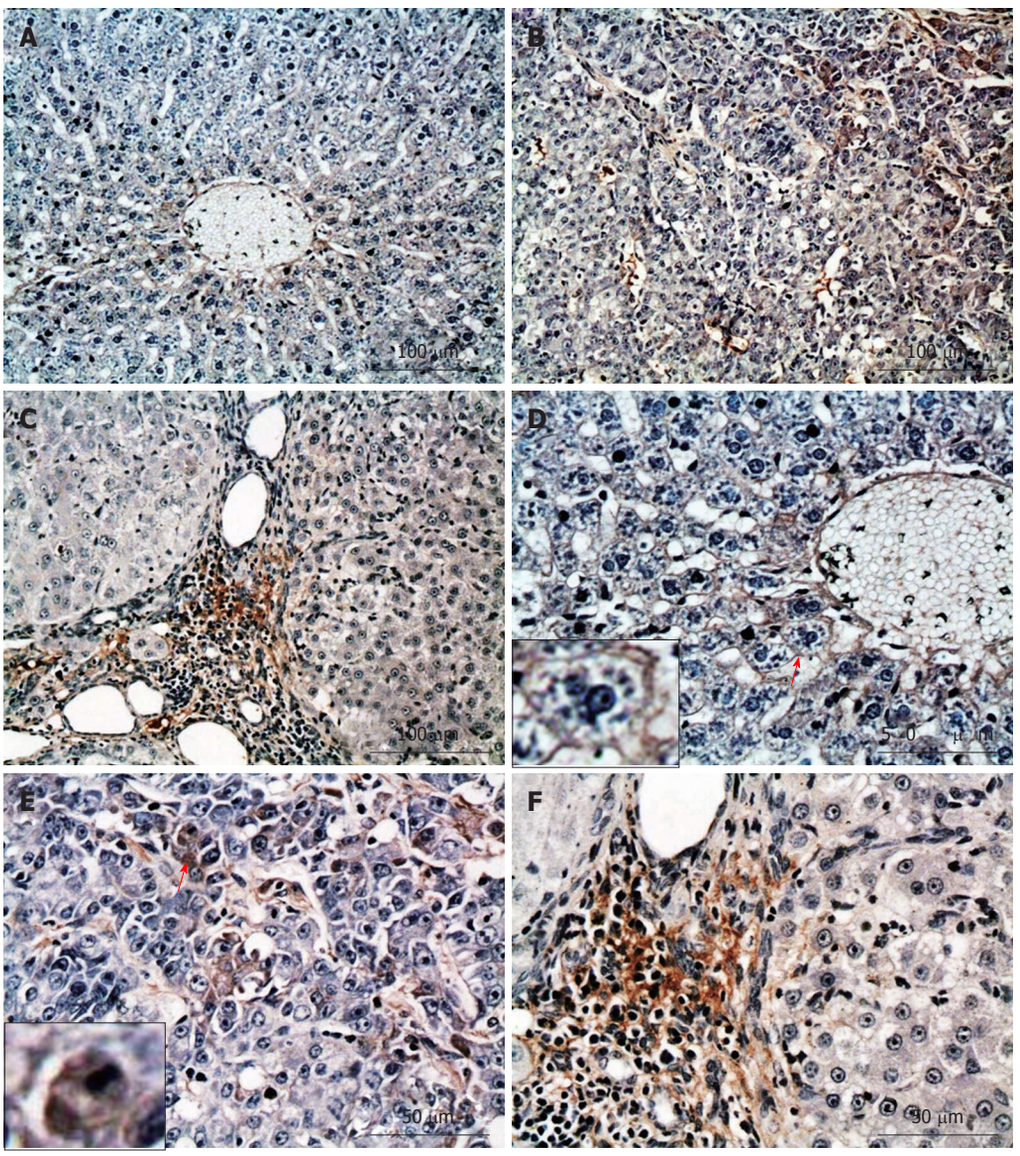

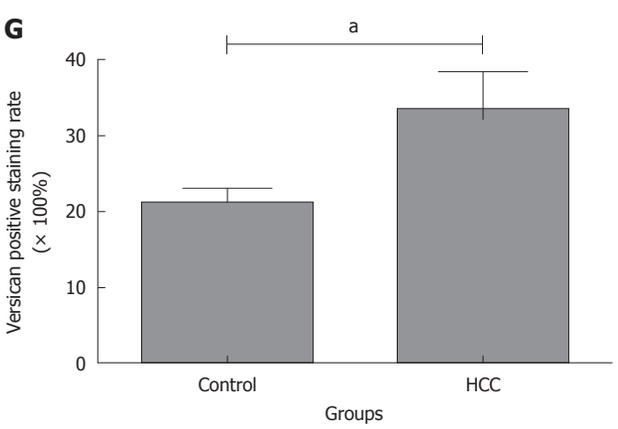

Figure 6 Immunochemical staining for versican in rat liver tissues. Versican positive staining was dark red. A-F: Most of hepatocytes were negatively stained in control group (A and D), whereas more hepatoma cells in hepatocellular carcinoma (HCC) nodules were positively stained (B and E); however, the strongest versican positive staining was observed in the fibrosis septa between hepatoma nodules (C and F). Short red arrows: The cells are magnified in the small boxes; G: Comparison of the positive rate for versican staining in liver tissues between the control and HCC model groups. [a]$P < 0.05$.

with that in the normal liver tissues (0.29 ± 0.01 and 0.26 ± 0.01, $P < 0.05$, Figure 8F). Interestingly, there was no decorin positive staining in the portal areas and fibrous tissue septa between the tumor nodules (Figure 8B and D).

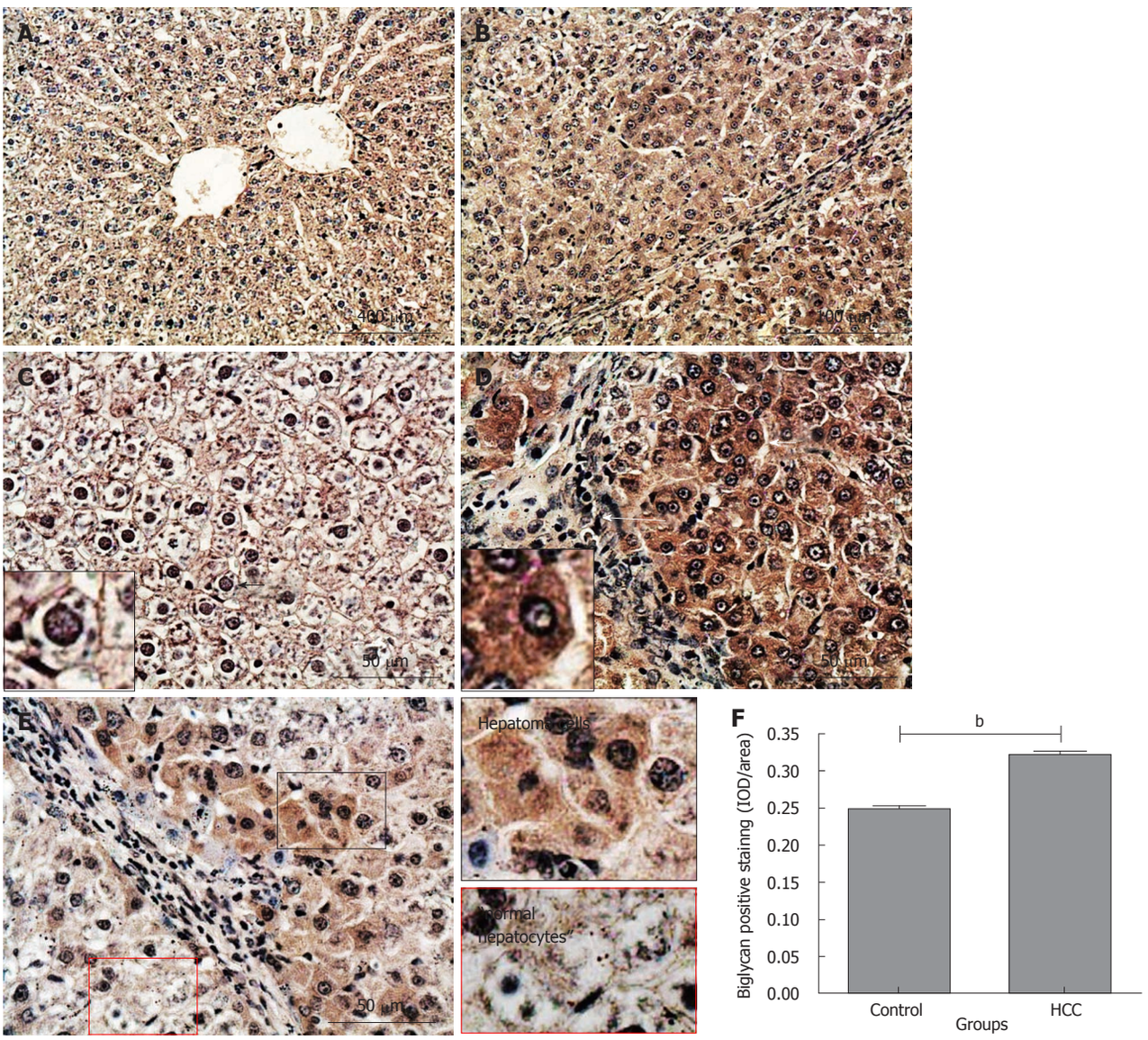

Figure 7 Immunochemical staining for biglycan in rat liver tissues. Biglycan positive staining was dark red. A and C: Control group; B, D and E: Hepatocellular carcinoma (HCC) model group. Long white arrow: **Fibrous tissue septa; short black and white arrows: The cells are magnified in the small boxes; E: Areas in black and** red boxes are magnified in left column; F: Comparison of the average integrated optical density (IOD) in biglycan positive staining in liver tissues between the control and HCC model groups ($^{b}P < 0.001$). IOD/area: **Integrated optical density per stained area.**

There was no positive staining for keratocan or lumican in rat liver tissues

The expression of keratocan and lumican was also investigated. Consistent with the KS negative staining results, there was no or very weak keratocan or lumican staining in these liver tissues, either from the control or HCC model group (data not shown).

DISCUSSION

The abnormally high expression of CS GAGs in HCC tissues has been known for a long time[16,17] although little is known about the biological mechanisms underlying their increased presence. Interestingly, an accumulation of CS GAG expression has also been observed in other physiological and pathological processes involved in liver development and metabolism. For example, in neonatal liver where premature hepatocytes (hepatic stem cells) still remain as an undifferentiated phenotype, much higher CS GAGs were observed when compared with that in the postnatal liver tissues[13]. Similarly, there is a transient accumulation of CS GAGs during liver regeneration after partial hepatectomy[13] and active fibrosis[24]. All of these examples demonstrate that CSPGs are involved in embryogenesis, regeneration and carcinogenesis of liver. One of the crucial events occurring within these biological processes is the epithelial mesenchymal transition (EMT), a complex molecular and cellular transformation of cell phenotype from differentiated characteristics (mature epithelial cells) to undifferentiated mesenchymal (stem/progenitor cells) features. During this process, cells acquire motility, enhanced migratory capacity/invasiveness[25], and become more stem cell-like[26]. Interestingly, increased production of ECM components such as CS

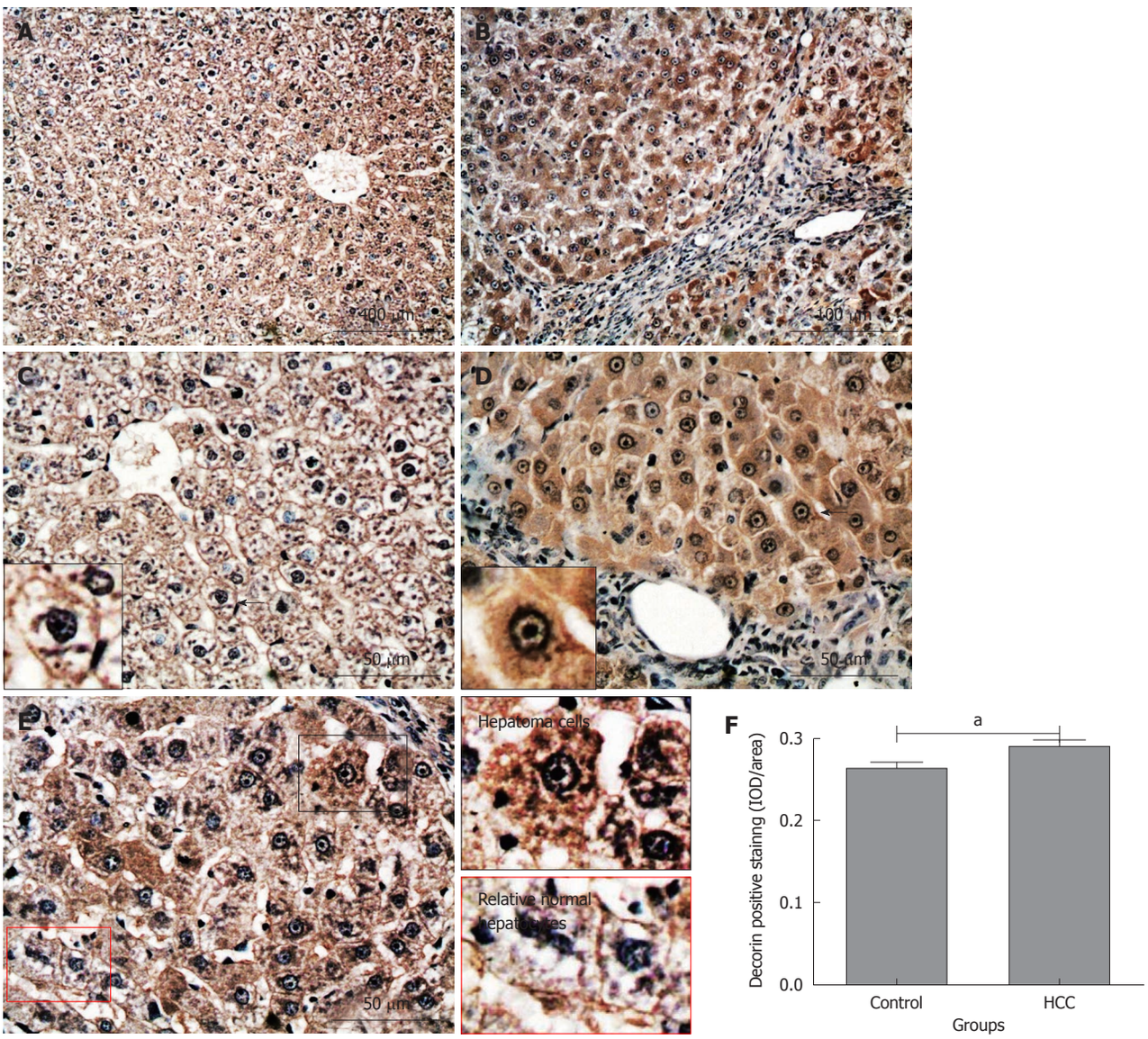

Figure 8 Immunochemical staining for decorin in rat liver tissues. Decorin positive staining was dark red. A and C: Control group; B, D and E: Hepatocellular carcinoma (HCC) model group. Short black arrows: The cells are magnified in the small boxes; E: Areas in black and red boxes are magnified in left column; F: Comparison of the average integrated optical density (IOD) in decorin positive staining in liver tissues between the control and HCC model groups ($^aP < 0.05$). IOD/area: Integrated optical density per stained area.

GAGs has been observed during this process[8,27], demonstrating that *de novo* CSPG expression may play a pivotal role during the cell phenotype transformation, notably initiating the development of HCC. However, it is still unclear what the precise CSPG expression patterns are in the hepatoma cells and their relationship with HCC development.

In this study, the Toluidine blue staining results indicated that there was more sGAG content in HCC tissues than that in the normal liver tissues from the control group, which is consistent with previous studies[16,17]. Our further immunostaining with CS/DS, HS and KS antibodies demonstrated that there was a significant increase in CS/DS and HS but not KS GAG expression in HCC tissues. The weak expression of KS GAG in both normal liver and HCC tissues is consistent with the very low staining patterns for keratocan and lumican, two major KSPGs expressed in the other tissues. A recent study performed on human HCC tissues[28], indicated that KSPGs were not involved in HCC development. Therefore, the increased sGAG content in HCC tissues must be induced by the enhanced production and accumulation of CS/DS and/or HSPGs, which is confirmed by our CS/DS and HS GAG staining. Previous studies have reported the expression of several HSPGs including glypican-3[29], syndecan-4[30] and perlecan[31] are increased in HCC tissues, which coincides with our HS staining results. However, little is known for the expression patterns of specific CSPGs in HCC, therefore our following investigation was mainly focused on CSPG expression.

Aggrecan gene expression has been previously reported in liver tissues[14,22]. Our results demonstrate, for the first time at a protein level, the positive expression of aggrecan in liver tissues, which was mainly localized on

the cell membrane and/or pericellular matrix in normal hepatocytes. However, in the HCC model group there was much stronger aggrecan staining in the cytoplasm, the cell membranes and/or pericellular matrix in HCC hepatoma cells, indicating an elevated aggrecan production and accumulation in HCC tissues. The function of this increased aggrecan presence is not clear but a previous study has suggested that the expression of aggrecan in tumors may be a result of EMT[27]. Moreover, aggrecan production is mediated by different growth factors such as transforming growth factor β in hepatocytes[22,32], which has been identified as a promoter for both HCC-related fibrosis and angiogenesis[32,33]. Interestingly, there was very low aggrecan expression in the fibrous tissue septa between hepatoma nodules, consistent with previous studies showing that the formation of fibrous septa arises from myofibroblasts[34], which have a low expression of CS/DS PGs[35].

In contrast to the increased aggrecan expression, versican content in hepatoma cells was variable with the most intensive staining mainly localized in the ECM of fibrous septa between hepatoma nodules. This finding is novel as little is known about versican expression in HCC tissues. Interestingly, versican expression was observed around the central veins and portal areas, illustrating there may be a close relationship between versican and HCC metastases. This is consistent with previous studies, where an elevated expression of versican was observed in the ECM of other tumor tissues including breast[36] and prostate[37], and correlated with metastases[38]. The mechanism as to how versican promotes metastases is not clear. However, the deposition of versican in the tumor stroma, particularly in the hyaluronic acid rich region, will lead to the structural aggregation of tumor matrix and modulation of cellular attachment and motility, therefore supporting cancer cell growth, proliferation, migration and differentiation, all processes vital for tumor development and metastases[5,36].

Both biglycan and decorin are the members of the small leucine-rich proteoglycan family. They are usually associated with growth factor binding[4] and collagen fibrillogenesis[39,40]. Therefore, it is not surprising that an elevated biglycan and decorin expression was observed during liver fibrosis[10,41,42]. However, our results showed that the major positive staining of decorin and biglycan was localized in the hepatoma cells instead of fibrosis septa between hepatoma nodules, suggesting that the expression of biglycan and decorin may play different roles in HCC occurrence and liver fibrosis. The association between biglycan and HCC has not been previously reported; however, elevated expression of biglycan may correlate with the aggressiveness and poor prognosis of the other cancers[43]. Varied evidence for the changes in decorin expression in HCC tissues has been previously reported. Kovalszky *et al*[17] and Lai *et al*[44] have found that decorin expression was elevated in HCC tissues. In contrast, Miyasaka *et al*[45] showed that there was a decline in decorin gene expression in HCC. The difference may arise from the different stages of HCC, as previous studies have showed that decorin can be either pro-angiogenic or anti-angiogenic in tumors[46]. The precise contributions of biglycan and decorin metabolism during HCC occurrence and metastases have not yet been elucidated. However, the ability of these proteins to interact with the other matrix components and induce ECM remodeling[47] as well as increasing cell proliferation and migration[48] highlights them as an important PG subsets involved in tumor formation and metastases. Alternatively, the increased biglycan and decorin expression may also be a consequence of EMT of hepatoma cells, because a recent study reported higher biglycan and decorin expression levels during a Ras-induced EMT in MDCK cells[49]. Clearly, further studies for the roles of biglycan and decorin in hepatocarcinogenesis are warranted.

Much less is known about the precise role that CSPGs play in the HCC induction and metastases. CSPGs are ubiquitous components of ECM and cell surface, therefore can predominantly interact with a wide variety of key molecules, such as growth factors, cytokines, chemokines, adhesion molecules, and lipoproteins. These interactions regulate biological processes including signaling, cell differentiation, cell-cell or cell-matrix interactions and morphogenesis[50]. In this study, using histological staining, we found a significant increase in the sGAG content in DEN-induced HCC tissues when compared with the normal rat liver tissues from the control group and this increased sGAG content in tumor tissue was mainly induced by elevated expression in CS/DS and HS but not KS GAGs. We further demonstrated that the expression of several CSPGs including aggrecan, versican, biglycan and decorin was elevated in HCC tissues. To our knowledge, this is the first systematical study demonstrating the elevated CSPGs expression in HCC tissues. The experimental data shown here expands our knowledge of the relationships between CS/DS PGs and HCC, and other liver diseases.

COMMENTS

Background

Proteoglycans (PGs) are macromolecules consisting of one or several polysaccharide chains of the glycosaminoglycan (GAG), which covalently attached to a variety of core proteins. They are widely expressed in cells and extracellular matrix in various tissues including liver. According to the difference in GAG side chains, PGs can be categorized as chondroitin sulphate PG (CSPG) and heparan sulphate PG, *etc*. PGs have been found to play a critical role in different malignant tumor progression. However, the effect of PGs on cancer is variable, which can range from stimulatory to inhibitory, depending on their core proteins and GAG types, the sources and stages of cancers and the tumor localizations.

Research frontiers

Previous studies have shown that the expression of CS GAG was increased in hepatocellular carcinoma (HCC) tissues, and inhibition of CS GAG expression in HCC cell line partially abrogates cell ability of migration *in vitro*. This illustrated that CSPGs may play a pivotal role in the occurrence, progression and metastasis of HCC and thereby they may be used as potential markers and treatment target for HCC. The hotspot in this area is their temporal and spatial expression and the mechanism how they are involved in the onset, development and metastasis of HCC.

Innovations and breakthroughs

The authors investigated the expression pattern of different CSPGs including aggrecan, versican, decorin, biglycan in the liver tissues from a rat HCC model

established using N-diethylnitrosamine (DEN). This is the first systematical study demonstrating the elevated CSPGs expression in HCC tissues.

Applications

The study results suggest that the CSPGs could be potential therapeutic targets and clinical biomarkers for HCC in humans in the future.

Terminology

PG is a kind of macromolecule units consists of a "core protein" with one or more covalently attached GAG chain(s); GAGs are long unbranched polysaccharides consisting of a repeating disaccharide unit; Chondroitin sulfate is a sulfated GAG composed of a chain of alternating sugars (N-acetylgalactosamine and glucuronic acid).

Peer review

This is a good descriptive study in which authors investigate the expression of PGs in rats with DEN-induced HCC. The results are interesting and suggest that CSPGs are potential therapeutic targets and clinical biomarkers for HCC.

REFERENCES

1 **Caterson B**. Fell-Muir Lecture: chondroitin sulphate glycosaminoglycans: fun for some and confusion for others. *Int J Exp Pathol* 2012; **93**: 1-10
2 **Maeda N**, Ishii M, Nishimura K, Kamimura K. Functions of chondroitin sulfate and heparan sulfate in the developing brain. *Neurochem Res* 2011; **36**: 1228-1240
3 **Wegrowski Y**, Maquart FX. Involvement of stromal proteoglycans in tumour progression. *Crit Rev Oncol Hematol* 2004; **49**: 259-268
4 **Schaefer L**, Schaefer RM. Proteoglycans: from structural compounds to signaling molecules. *Cell Tissue Res* 2010; **339**: 237-246
5 **Theocharis AD**, Skandalis SS, Tzanakakis GN, Karamanos NK. Proteoglycans in health and disease: novel roles for proteoglycans in malignancy and their pharmacological targeting. *FEBS J* 2010; **277**: 3904-3923
6 **Kirn-Safran C**, Farach-Carson MC, Carson DD. Multifunctionality of extracellular and cell surface heparan sulfate proteoglycans. *Cell Mol Life Sci* 2009; **66**: 3421-3434
7 **ten Dam GB**, van de Westerlo EM, Purushothaman A, Stan RV, Bulten J, Sweep FC, Massuger LF, Sugahara K, van Kuppevelt TH. Antibody GD3G7 selected against embryonic glycosaminoglycans defines chondroitin sulfate-E domains highly up-regulated in ovarian cancer and involved in vascular endothelial growth factor binding. *Am J Pathol* 2007; **171**: 1324-1333
8 **Soltermann A**, Tischler V, Arbogast S, Braun J, Probst-Hensch N, Weder W, Moch H, Kristiansen G. Prognostic significance of epithelial-mesenchymal and mesenchymal-epithelial transition protein expression in non-small cell lung cancer. *Clin Cancer Res* 2008; **14**: 7430-7437
9 **Asimakopoulou AP**, Theocharis AD, Tzanakakis GN, Karamanos NK. The biological role of chondroitin sulfate in cancer and chondroitin-based anticancer agents. *In Vivo* 2008; **22**: 385-389
10 **Meyer DH**, Krull N, Dreher KL, Gressner AM. Biglycan and decorin gene expression in normal and fibrotic rat liver: cellular localization and regulatory factors. *Hepatology* 1992; **16**: 204-216
11 **Gressner AM**, Vasel A. Proteochondroitin sulfate is the main proteoglycan synthesized in fetal hepatocytes. *Proc Soc Exp Biol Med* 1985; **180**: 334-339
12 **Gressner AM**, Vasel A. Developmental changes of proteoglycan synthesis in rat liver and isolated hepatocytes. *Mech Ageing Dev* 1985; **31**: 307-327
13 **Yada T**, Koide N, Kimata K. Transient accumulation of perisinusoidal chondroitin sulfate proteoglycans during liver regeneration and development. *J Histochem Cytochem* 1996; **44**: 969-980
14 **Krull NB**, Gressner AM. Differential expression of keratan sulphate proteoglycans fibromodulin, lumican and aggrecan in normal and fibrotic rat liver. *FEBS Lett* 1992; **312**: 47-52
15 **Kovalszky I**, Pogany G, Molnar G, Jeney A, Lapis K, Karacsonyi S, Szecseny A, Iozzo RV. Altered glycosaminoglycan composition in reactive and neoplastic human liver. *Biochem Biophys Res Commun* 1990; **167**: 883-890
16 **Kojima J**, Nakamura N, Kanatani M, Omori K. The glycosaminoglycans in human hepatic cancer. *Cancer Res* 1975; **35**: 542-547
17 **Kovalszky I**, Schaff Z, Jeney A. Potential markers (enzymes, proteoglycans) for human liver tumors. *Acta Biomed Ateneo Parmense* 1993; **64**: 157-163
18 **Kiernan JA**. Histological and Histochemical Methods: Theory and Practice. 4th ed. Oxford: Scion Publishing Ltd., 2008
19 **Hayes AJ**, Hughes CE, Caterson B. Antibodies and immunohistochemistry in extracellular matrix research. *Methods* 2008; **45**: 10-21
20 **Ivarsson K**, Myllymäki L, Jansner K, Bruun A, Stenram U, Tranberg KG. Heat shock protein 70 (HSP70) after laser thermotherapy of an adenocarcinoma transplanted into rat liver. *Anticancer Res* 2003; **23**: 3703-3712
21 **Edmondson HA**, Steiner PE. Primary carcinoma of the liver: a study of 100 cases among 48,900 necropsies. *Cancer* 1954; **7**: 462-503
22 **Gressner AM**, Krull N, Bachem MG. Regulation of proteoglycan expression in fibrotic liver and cultured fat-storing cells. *Pathol Res Pract* 1994; **190**: 864-882
23 **Hayes AJ**, Tudor D, Nowell MA, Caterson B, Hughes CE. Chondroitin sulfate sulfation motifs as putative biomarkers for isolation of articular cartilage progenitor cells. *J Histochem Cytochem* 2008; **56**: 125-138
24 **Galambos JT**. Acid mucopolysaccharides and cirrhosis of the liver. *Gastroenterology* 1966; **51**: 65-74
25 **Kalluri R**, Weinberg RA. The basics of epithelial-mesenchymal transition. *J Clin Invest* 2009; **119**: 1420-1428
26 **Polyak K**, Weinberg RA. Transitions between epithelial and mesenchymal states: acquisition of malignant and stem cell traits. *Nat Rev Cancer* 2009; **9**: 265-273
27 **Erdélyi I**, van Asten AJ, van Dijk JE, Nederbragt H. Expression of versican in relation to chondrogenesis-related extracellular matrix components in canine mammary tumors. *Histochem Cell Biol* 2005; **124**: 139-149
28 **Miyamoto T**, Ishii K, Asaka R, Suzuki A, Takatsu A, Kashima H, Shiozawa T. Immunohistochemical expression of keratan sulfate: a possible diagnostic marker for carcinomas of the female genital tract. *J Clin Pathol* 2011; **64**: 1058-1063
29 **Capurro M**, Wanless IR, Sherman M, Deboer G, Shi W, Miyoshi E, Filmus J. Glypican-3: a novel serum and histochemical marker for hepatocellular carcinoma. *Gastroenterology* 2003; **125**: 89-97
30 **Charni F**, Friand V, Haddad O, Hlawaty H, Martin L, Vassy R, Oudar O, Gattegno L, Charnaux N, Sutton A. Syndecan-1 and syndecan-4 are involved in RANTES/CCL5-induced migration and invasion of human hepatoma cells. *Biochim Biophys Acta* 2009; **1790**: 1314-1326
31 **Roskams T**, De Vos R, David G, Van Damme B, Desmet V. Heparan sulphate proteoglycan expression in human primary liver tumours. *J Pathol* 1998; **185**: 290-297
32 **Benetti A**, Berenzi A, Gambarotti M, Garrafa E, Gelati M, Dessy E, Portolani N, Piardi T, Giulini SM, Caruso A, Invernici G, Parati EA, Nicosia R, Alessandri G. Transforming growth factor-beta1 and CD105 promote the migration of hepatocellular carcinoma-derived endothelium. *Cancer Res* 2008; **68**: 8626-8634
33 **Dooley S**, Weng H, Mertens PR. Hypotheses on the role of transforming growth factor-beta in the onset and progression of hepatocellular carcinoma. *Dig Dis* 2009; **27**: 93-101
34 **Desmoulière A**, Guyot C, Gabbiani G. The stroma reaction myofibroblast: a key player in the control of tumor cell behavior. *Int J Dev Biol* 2004; **48**: 509-517
35 **Gressner AM**. Proliferation and transformation of cultured

liver fat-storing cells (perisinusoidal lipocytes) under conditions of beta-D-xyloside-induced abrogation of proteoglycan synthesis. *Exp Mol Pathol* 1991; **55**: 143-169
36 **Suwiwat S**, Ricciardelli C, Tammi R, Tammi M, Auvinen P, Kosma VM, LeBaron RG, Raymond WA, Tilley WD, Horsfall DJ. Expression of extracellular matrix components versican, chondroitin sulfate, tenascin, and hyaluronan, and their association with disease outcome in node-negative breast cancer. *Clin Cancer Res* 2004; **10**: 2491-2498
37 **Ricciardelli C**, Mayne K, Sykes PJ, Raymond WA, McCaul K, Marshall VR, Horsfall DJ. Elevated levels of versican but not decorin predict disease progression in early-stage prostate cancer. *Clin Cancer Res* 1998; **4**: 963-971
38 **Yip GW**, Smollich M, Götte M. Therapeutic value of glycosaminoglycans in cancer. *Mol Cancer Ther* 2006; **5**: 2139-2148
39 **Schönherr E**, Witsch-Prehm P, Harrach B, Robenek H, Rauterberg J, Kresse H. Interaction of biglycan with type I collagen. *J Biol Chem* 1995; **270**: 2776-2783
40 **Sugars RV**, Milan AM, Brown JO, Waddington RJ, Hall RC, Embery G. Molecular interaction of recombinant decorin and biglycan with type I collagen influences crystal growth. *Connect Tissue Res* 2003; **44** Suppl 1: 189-195
41 **Gallai M**, Kovalszky I, Knittel T, Neubauer K, Armbrust T, Ramadori G. Expression of extracellular matrix proteoglycans perlecan and decorin in carbon-tetrachloride-injured rat liver and in isolated liver cells. *Am J Pathol* 1996; **148**: 1463-1471
42 **Högemann B**, Edel G, Schwarz K, Krech R, Kresse H. Expression of biglycan, decorin and proteoglycan-100/CSF-1 in normal and fibrotic human liver. *Pathol Res Pract* 1997; **193**: 747-751
43 **Wang B**, Li GX, Zhang SG, Wang Q, Wen YG, Tang HM, Zhou CZ, Xing AY, Fan JW, Yan DW, Qiu GQ, Yu ZH, Peng ZH. Biglycan expression correlates with aggressiveness and poor prognosis of gastric cancer. *Exp Biol Med* (Maywood) 2011; **236**: 1247-1253
44 **Lai KK**, Shang S, Lohia N, Booth GC, Masse DJ, Fausto N, Campbell JS, Beretta L. Extracellular matrix dynamics in hepatocarcinogenesis: a comparative proteomics study of PDGFC transgenic and Pten null mouse models. *PLoS Genet* 2011; **7**: e1002147
45 **Miyasaka Y**, Enomoto N, Nagayama K, Izumi N, Marumo F, Watanabe M, Sato C. Analysis of differentially expressed genes in human hepatocellular carcinoma using suppression subtractive hybridization. *Br J Cancer* 2001; **85**: 228-234
46 **Iozzo RV**, Moscatello DK, McQuillan DJ, Eichstetter I. Decorin is a biological ligand for the epidermal growth factor receptor. *J Biol Chem* 1999; **274**: 4489-4492
47 **Tufvesson E**, Westergren-Thorsson G. Biglycan and decorin induce morphological and cytoskeletal changes involving signalling by the small GTPases RhoA and Rac1 resulting in lung fibroblast migration. *J Cell Sci* 2003; **116**: 4857-4864
48 **Kinsella MG**, Bressler SL, Wight TN. The regulated synthesis of versican, decorin, and biglycan: extracellular matrix proteoglycans that influence cellular phenotype. *Crit Rev Eukaryot Gene Expr* 2004; **14**: 203-234
49 **Mathias RA**, Chen YS, Wang B, Ji H, Kapp EA, Moritz RL, Zhu HJ, Simpson RJ. Extracellular remodelling during oncogenic Ras-induced epithelial-mesenchymal transition facilitates MDCK cell migration. *J Proteome Res* 2010; **9**: 1007-1019
50 **Wegrowski Y**, Milard AL, Kotlarz G, Toulmonde E, Maquart FX, Bernard J. Cell surface proteoglycan expression during maturation of human monocytes-derived dendritic cells and macrophages. *Clin Exp Immunol* 2006; **144**: 485-493

S- Editor Lv S **L- Editor** Ma JY **E- Editor** Zheng XM